

SYNCHROTRON RADIATION TEST VALIDATIONS OF EUROPEAN XFEL MCP BASED DETECTORS AT DORIS BEAMLINE BW1

Evgeny Syresin, Oleg Brovko, Alexander Grebentsov, Alexey Shabunov, Nikolaj Zamjatin,
Joint Institute for Nuclear Research, Dubna, Russia
Mikhail Yurkov, Dmitriy Novikov DESY, Hamburg, Germany
Wolfgang Freund, Jan Grünert, Harald Sinn, European XFEL GmbH, Hamburg, Germany
Pavel Hedbavny, Tomas Fiala, Roman Basta, Vakuu Praha, Prague, Czech Republik

Abstract

Radiation detectors based on micro channel plates (MCP) are planned for installation at the European XFEL. Main purpose of these detectors is searching a signature of lasing and further fine tuning of the FEL process. Detectors operate in a wide dynamic range from the level of spontaneous emission to the saturation level (between a few nJ and 25 mJ), and in a wide wavelength range from 0.05 nm to 0.4 nm for SASE1 and SASE2, and from 0.4 nm to 4.43 nm for SASE3. Photon pulse energies are measured with traditional MCP with anode and with photodiode. The photon beam image is measured by MCP imager with phosphor screen anode.

The SR tests validation of the MCP-based detector applied for XFEL SASE1 and SASE2 were performed at the DORIS beamline BW1 and photon energy of 8.5-12.4 keV. The absolute measurements of a photon pulse energy of 0.03 nJ and larger for hard X-ray radiation were performed with application of MCP and photodiode detectors. Pulse-to-pulse photon energy measurements with MCPs and a JINR silicon photo detector were done with 192 ns and 96 ns repetition intervals. The SR beam imaging measurement at X-ray irradiation was performed at test validation experiments.

DESIGN OF THE DETECTOR

An important task of the photon beam diagnostics at the European XFEL is providing reliable tools for measurements aiming at the search for and fine tuning of the FEL creating SASE process (Self Amplified Spontaneous Emission). The problem of finding SASE amplification is crucial for the XFEL because of a large synchrotron radiation background. This requires a detector with a wide dynamic range, controllable tuning to the required wavelength range, and suppression of the unwanted radiation background. The JINR-XFEL collaboration manufactured MCP-based photon detectors as a primary tool for the search for and fine tuning of the SASE process. Three MCP devices [1,2] will be installed, one after each SASE undulator of the European XFEL (SASE1, SASE2, and SASE3).

Three different tasks can be fulfilled with the XFEL MCP-based photon detectors [1,2]: study of the initial stage of the SASE regime; measurement of the photon pulse energy; and measurement of the photon beam image. The MCP detector will resolve each individual

pulse at a repetition rate of 4.5 MHz. The following wavelength ranges are to be covered by three MCP stations: 0.05-0.4 nm for MCP1 and MCP2, 0.4-4.43 nm for MCP3.

MCP detectors for SASE1 and SASE2 (Fig.1) are installed after the deflecting mirrors [3-5]. The offset mirrors are used for two distinctive and separate purposes: firstly during early commissioning they cutoff high harmonics of spontaneous radiation and improve the ratio of FEL/spontaneous intensity, secondly they are used as additional attenuators of the radiation intensity. The diamond attenuator and the Ce:YAG screen are installed in front of the first carbon coated offset mirror. The attenuation range of the mirrors combined with the diamond plate attenuators is about 10^3 - 10^4 . The dynamic range of the MCP is 10^3 - 10^4 .

The MCP detector for SASE1&SASE2 consists of a silicon photodiode, three MCPs equipped with an anode as a pulse energy monitor and one MCP detector for imaging the photon beam. The first MCP detector port houses one silicon photodiode and two F4655 Hamamatsu MCPs, 18 mm in diameter. The silicon photodiode and one MCP F4655 are shown in Fig.2 for prototype of the MCP detector. The PM 100-250 3D vacuum manipulator displaces these MCPs in the horizontal direction in a range of 250 mm. The range of vertical displacement is ± 2.5 cm relative to the beam axis.

The second detector port houses two MCPs: F4655 for measurement of the pulse energies, and the beam observation system (BOS) MCP (model BOS-40-IDA-CH/P-47) of 40 mm diameter with a phosphor screen. The BOS MCP is set at an angle of 45° with respect to the photon beam and a viewport allows imaging onto a CCD. The MCP detector for SASE3 will have an additional port with a movable semi-transparent mesh and wire targets to produce scattered FEL radiation similar to those used at FLASH [6-9].

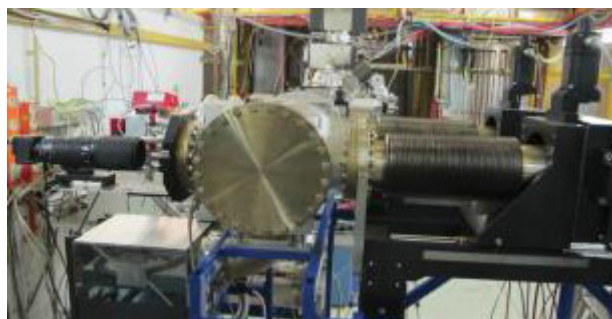


Figure 1: View of SASE1 and SASE2 MCP detector during the DORIS test validation.



Figure 2: Silicon photodiode and MCP F4655 in the MCP detector prototype.

TEST VALIDATION EXPERIMENTS WITH MCP DETECTOR

The calibration of the MCP detector was realized in X-ray and UV wavelength range before installation of this detector in the XFEL tunnel. Initially the F4655 Hamamatsu MCPs were calibrated with a UV lamp. The MCP 1 and MCP 2 amplification gains are shown in Fig. 3. The MCP gain corresponds to 4 orders of magnitude. Previous experience from FLASH with similar F4655 Hamamatsu MCPs shows that when the light intensity is high, the applied voltage needs to be reduced, and below 1400 V the space charge effects in MCP channels start to play a significant role [6-9].

Further validation tests with the MCP detector were performed at DORIS BW1 beamline. The absolute measurements of a photon pulse energy of 0.03 nJ and larger for hard X-ray radiation were performed with application of MCP and photodiode detectors.

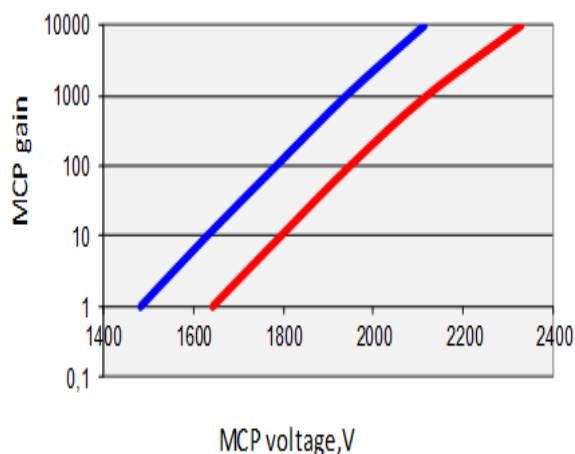


Figure 3: Dependence of MCP1 (blue line) and MCP2 (red line) gains on MCP voltage.

The photon flux was in a range of $2 \cdot 10^{11}$ ph/s to $2 \cdot 10^8$ ph/s. The SR measurements were performed at photon energies of 8.5 to 12.4 keV. Variation of photon energy was done with the BW1 undulator gap. Vacuum pressure in the MCP-detector UHV chamber was 5×10^{-9} mbar. The MCP entrance window is a 200 μ m thick beryllium foil. Pulse-to-pulse photon energy measurements with MCPs and a silicon photo detector were done with 192 ns and 96 ns repetition intervals. The SR beam imaging measurement under X-ray irradiation was performed at test validation experiments. The X-ray beam image was measured by the MCP detector at a photon energy of 9.66 keV. The MCP beam observation system with a phosphor screen can be effectively used for search of SASE mode starting from spontaneous emission.

The gas ionization monitor (GIM) was used for measurement of the SR photon flux. Dependence of the MCP signal on the GIM signal is shown in Fig.4. The linear behavior of the MCP 1 signal versus the gas ionization monitor signal is observed at an MCP1 voltage of 1.85 kV and below.

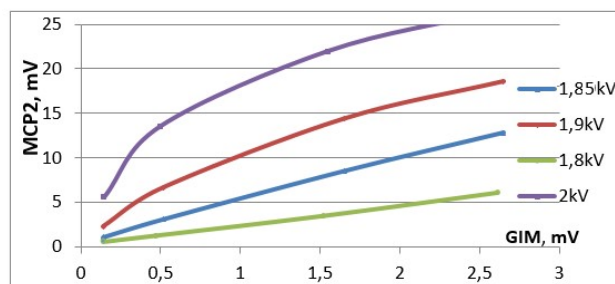


Figure 4: Dependence of MCP2 signal on gas ionization chamber signal at different MCP 2 voltages.

An essential influence of secondary ions produced by X-rays in the MCP chamber at a pressure of 5×10^{-9} mbar was observed during MCP operation in DORIS BW1. The nonlinear dependence of the MCP signal on X-ray beam intensity was measured at MCP voltages higher than 1.9 kV (Fig.4). When the ion pump was switched on or off ,

Content from this work may be used under the terms of the CC BY 3.0 licence (© 2014). Any distribution of this work must maintain attribution to the author(s), title of the work, publisher, and DOI.

we did not see any difference of the ion input in the MCP operation. Therefore, we assume that the X-rays produce secondary ions by ionization of residual gas atoms.

MCP gain versus photon energy of UV and X-ray radiations is given in Fig.5 where the MCP voltage was increased from 1.8 to 1.85 kV. In accordance to the UV calibration (Fig.5) the MCP gain corresponds to 2.1 at MCP2 voltage increase from 1.8 to 1.85 kV. For X-ray radiation at photon energy 8.5-12.4 keV this gain varies in a range of 1.7 to 2.1.

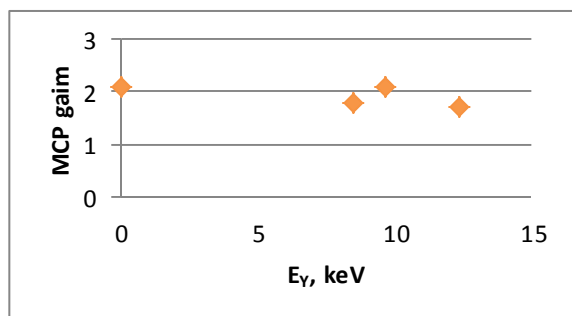


Figure 5: Dependence of MCP2 gain on photon energy at increase of MCP voltage from 1.8 kV to 1.85 kV.

The ratio of the MCP2 signal to SR pulse energy corresponds to 0.11-0.16 V/nJ at photon energy of 8.5-12.4 keV and MCP voltage of 1.8 kV.

The XFEL micro pulse energy of 1 mJ should produce an MCP amplitude signal of 1.2 V for a MCP voltage of 1.5 kV (assuming an MCP gain reduction of 10^{-2} in comparison to 1.8 kV MCP voltage) and attenuation factor of XFEL radiation $R=10^{-3}$ in accordance with SR test measurements of the calibration ratio 0.12 V/nJ at MCP voltage 1.8 kV.

The SR photon flux was measured by a silicon photodiode and GIM. Linear dependence of the photodiode signal in pulsed mode versus the gas ionization monitor signal is presented in Fig.6. Maximum photodiode current of 105 μ A corresponds to SR photon flux of $2.4 \cdot 10^{11}$ ph/s.

Time structure of SR pulses at a frequency of about 10 MHz was observed in the measurements with both MCP and silicon photodiode (Fig.7).

The X-ray beam image was measured by MCP detector at intensity higher than $4 \cdot 10^7$ ph/s at a photon energy of 9.66 keV. The MCP beam observation system with a phosphor screen is effectively used for the search of the SR photon beam position.

However at SR tests the measured X-ray beam size at small slits of 0.2-0.4 mm was about 1.8 -2 mm caused by low contrast resolution of the phosphor screen and image spot spreading. The MCP imager can be applied for search of the SASE photon beam spot; however it cannot be used for detailed measurements of the spot shape and substructure.

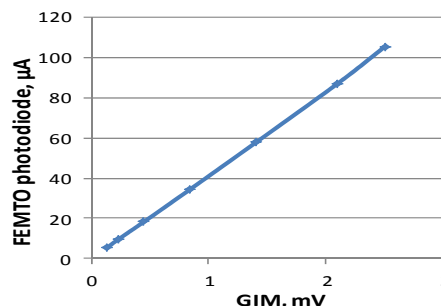


Figure 6: Dependence of XFEL Canberra PIPS diode current on gas ionisation monitor (GIM) signal at $E_\gamma=9.66$ keV.



Figure 7: The time structure of MCP1 (upper signal) and photodiode (lower signal).

ACKNOWLEDGEMENT

The MCP detector project is realized in the frame of the XFEL-JINR R03 Contract for WP74 of the European XFEL

REFERENCES

- [1] E. Syresin et al., IPAC11, 1106 (2011).
- [2] O.Brovko et al, RUPAC12, 572 (2012).
- [3] J. Grünert, FEL09 146 (2009).
- [4] H. Sinn et al, FEL10, 683 (2010).
- [5] H. Sinn et al., Conceptual Design Report X-ray Optics and Beam Transport, European XFEL (2011), 8.
- [6] B. Faatz et al., NIM A 483, 412 (2002).
- [7] A. Bytchkov et al., NIM A 528, 254 (2004),
- [8] W. Ackermann et al., Nature Photonics, 1, 336 (2007).
- [9] L. Bittner et al, FEL 07, 334 (2007).